

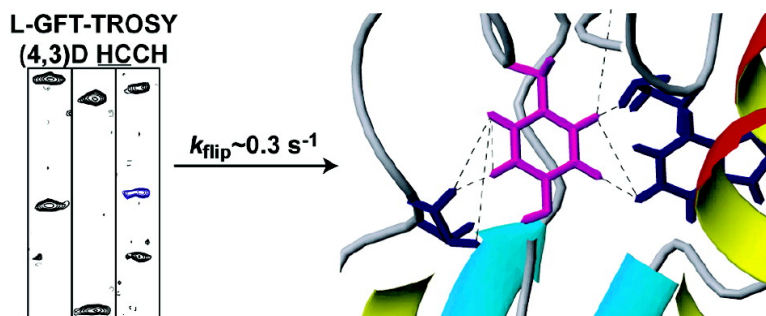
Communication

Probing Structure and Functional Dynamics of (Large) Proteins with Aromatic Rings: L-GFT-TROSY (4,3)D HCCH NMR Spectroscopy

Alexander Eletsky, Hanudatta S. Atreya, Gaohua Liu, and Thomas Szyperski

J. Am. Chem. Soc., **2005**, 127 (42), 14578-14579 • DOI: 10.1021/ja054895x • Publication Date (Web): 29 September 2005

Downloaded from <http://pubs.acs.org> on March 25, 2009



More About This Article

Additional resources and features associated with this article are available within the HTML version:

- Supporting Information
- Links to the 4 articles that cite this article, as of the time of this article download
- Access to high resolution figures
- Links to articles and content related to this article
- Copyright permission to reproduce figures and/or text from this article

[View the Full Text HTML](#)

Probing Structure and Functional Dynamics of (Large) Proteins with Aromatic Rings: L-GFT-TROSY (4,3)D HCCH NMR Spectroscopy

Alexander Eletsky, Hanudatta S. Atreya, Gaohua Liu, and Thomas Szyperski*

Department of Chemistry, State University of New York at Buffalo, Buffalo, New York 14260, Northeast Structural Genomics Consortium

Received July 21, 2005; E-mail: szypersk@chem.buffalo.edu

The rings of aromatic amino acids are valuable probes to study protein structure, dynamics, and folding by using nuclear magnetic resonance (NMR) spectroscopy. They are often part of a protein's molecular core and give rise to a large number of ^1H - ^1H nuclear Overhauser effects (NOEs),¹ as is required for high-quality structure determination. Ring flipping rates provide unique information on larger-amplitude motional modes which allow the rings to rotate about χ^2 .¹⁻³ Hence, NMR assignment of rings is of central importance for structural biology of proteins. HCCH spectroscopy⁴ employed in conjunction with NOE spectroscopy (NOESY) is most efficient,⁵ and four-dimensional (4D) HCCH is attractive due to limited shift dispersion of Phe rings.¹ Despite the tremendous importance, however, an implementation that provides 4D information while being suited for both *sensitivity* and *sampling* limited data collection⁶ is not available.

Here we present aromatic L-GFT and L-GFT-TROSY (4,3)D HCCH. *Sensitivity* is maximized by using (i) newly introduced longitudinal relaxation (L-)optimization⁷ for aromatic protons ($^1\text{H}^{\text{aromatic}}$), (ii) pulsed field gradient (PFG) selection of coherences with preservation of equivalent pathways (PEP),^{5,8} (iii) (semi-) constant time (*ct*) frequency labeling,⁵ and (iv) employment of transverse relaxation optimized spectroscopy (TROSY).⁹⁻¹¹ Rapid *sampling* is accomplished by use of G-matrix FT (GFT) NMR¹² combined^{13,14} with L-optimization, which thus serves to enhance sensitivity⁷ and/or shorten relaxation delays.¹³

$^1\text{H}^{\text{aromatic}}$ L-optimization is feasible since (i) $^1\text{H}^{\text{aromatic}}/^1\text{H}_2\text{O}$ and $^1\text{H}^{\text{aliphatic}}$ chemical shift ranges do not overlap, which enables selective "flipping" of $^1\text{H}^{\text{aliphatic}}/^1\text{H}_2\text{O}$ magnetization while $^1\text{H}^{\text{aromatic}}$ magnetization is along *z* and (ii) a large number of dipolar $^1\text{H}^{\text{aromatic}}-^1\text{H}^{\text{aliphatic}}$ and Tyr $^1\text{H}^{\text{aromatic}}-^1\text{H}^{\text{hydroxyl}}$ interactions can increase R_1 of $^1\text{H}^{\text{aromatic}}$. For 14 kDa protein Pfr13, a target of the Northeast Structural Genomics Consortium (NESG), we recorded a series of L- and *non-L-ct* 2D [^{13}C , ^1H]-HSQC/TROSY spectra (Figure S1) at 20 and 4 °C with varying relaxation delay between scans. PFG-PEP coherence selection⁸ was used.¹⁵ HSQC spectra were recorded at 20 °C, where the approximate isotropic correlation time for overall tumbling of Pfr13, τ_{iso} , is 8.5 ns. TROSY spectra with suppression of signal contributions from $^{13}\text{C}^{\text{aromatic}}$ polarization were acquired at 4 °C, where $\tau_{\text{iso}} = 12.5$ ns. Signal-to-noise (S/N) ratios were measured as a function of the relaxation delay between scans, t_{rel} , and divided by the square-root of the measurement time, t_{tot} , thus yielding SN_t , a measure for intrinsic sensitivity. A least-squares fit of

$$\text{SN}_t = A \frac{1 - \exp(-R_1(t_{\text{rel}} + t_{\text{acq}}))}{\sqrt{t_{\text{rel}} + t_{\text{acq}} + t_{\text{seq}}}} \quad (1)$$

to the experimental SN_t values yields $t_{\text{rel}}^{\text{opt}}$ at which, for a given proton, intrinsic sensitivity is maximal (Tables S1-S3). t_{acq} and t_{seq} represent the acquisition time and length of the pulsing period, respectively, while scaling factor *A* and effective longitudinal

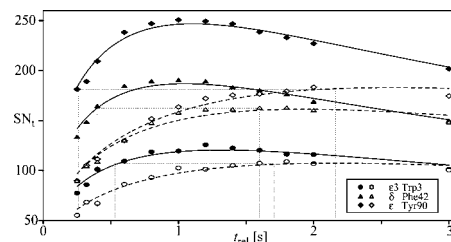


Figure 1. SN_t in *ct* 2D [^{13}C , ^1H]-HSQC versus t_{rel} for three peaks of protein Pfr13 (20 °C; 750 MHz). Filled (open) symbols and solid (dashed) lines correspond to spectra acquired *with* (*without*) L-optimization. Vertical lines at ~ 1.6 – 2.2 s indicate $t_{\text{rel}}^{\text{opt}}$ *without* L-optimization, and those at ~ 0.2 – 0.5 s indicate $t_{\text{rel}}^{\text{match}}$ (Table S1) where L-optimized congeners reach the same intrinsic sensitivity.

relaxation rate R_1 are fitted (Figure 1). Analysis of resolved peaks (Tables S1, S2) reveals that at 20 °C (4 °C) (i) the average $t_{\text{rel}}^{\text{opt}} = 1.9$ s (1.8 s) *without* is longer than the average $t_{\text{rel}}^{\text{opt}} = 1.1$ s (1.0 s) *with* L-optimization, and (ii) the average gain in intrinsic sensitivity arising at $t_{\text{rel}}^{\text{opt}}$ due to L-optimization (Figures 1, S2) is $\sim 20\%$ ($\sim 15\%$). For the L-optimized experiment acquired at $t_{\text{rel}}^{\text{match}} \sim 0.4$ – 0.6 s, intrinsic sensitivity matches the one of the *non-L* congener at its $t_{\text{rel}}^{\text{opt}}$, that is L-optimization allows one to reach the maximum sensitivity achieved *without* L-optimization at about 4-fold increased sampling speed.

Exploration of L-optimization with 2D NMR (Figures 1, S2; Tables S1-S3) enabled implementation of L-GFT-TROSY (4,3)D HCCH (Figure 2), which is based on highly efficient $^1\text{H}^{(1)}(t_1) \rightarrow ^{13}\text{C}^{(1)}(t_1) \rightarrow ^{13}\text{C}^{(2)}(t_2) \rightarrow ^1\text{H}^{(2)}(t_3)$ transfer via large $\{J\}^{13}\text{C}^{\text{aromatic}} - ^{13}\text{C}^{\text{aromatic}}\}$ (~ 50 Hz) and $\{J\}^1\text{H}^{\text{aromatic}} - ^{13}\text{C}^{\text{aromatic}}\}$ (~ 160 Hz) couplings. The shifts of $^1\text{H}^{(1)}$ and $^{13}\text{C}^{(1)}$ are jointly sampled in a GFT dimension. Frequency labeling with the shifts of $^1\text{H}^{(1)}$, $^{13}\text{C}^{(1)}$, and $^{13}\text{C}^{(2)}$ is accomplished within only ~ 11.6 – 13.5 ms during polarization transfer. Short maximal evolution times of ~ 4.5 ms suffice in the GFT dimension since peaks are dispersed over the sum of $^1\text{H}^{\text{aromatic}}$ and $^{13}\text{C}^{\text{aromatic}}$ spectral widths.¹³ At 4.5 ms *ct* delay, TROSY yields higher sensitivity only for large proteins ($\tau_{\text{iso}} > 23$ ns; Figure S4) but allows one to use $^{13}\text{C}^{(1)}$ polarization¹⁰ for acquiring central peaks^{12,17} without compromising on INEPT delays.¹⁸ These peaks provide (H)CCH information defining centers of peak pairs at $\Omega(^{13}\text{C}^{(1)}) \pm \Omega(^1\text{H}^{(1)})$ in basic spectra.

L-GFT-TROSY (4,3)D HCCH (data set "I") was recorded in 24 h with $t_{\text{rel}} = 1$ s ($t_{\text{rel}}^{\text{opt}}$ for Pfr13; Table S4) for 21 kDa protein HR41 (Figure 3; 25 °C; $\tau_{\text{iso}} \approx 11$ ns; 95% peak detection yield), an NESGC target for which data collection is *sensitivity* limited. For sensitivity comparison, L-GFT ("II"), GFT ("III"); $t_{\text{rel}} = 1.5$ s with presaturation of water line, and L-GFT-TROSY with 13.5 ms *ct* delay^{10,11} ("IV") were recorded. The relative sensitivity for *basic spectra* is $\sim 2.5:3.8:2.1:1$ (Table S5). Thus, at $\tau_{\text{iso}} \approx 11$ ns one has that (i) TROSY is $\sim 20\%$ less sensitive¹⁹ when also taking into account that ^{13}C polarization yields central peaks in TROSY (see Supporting Information), (ii) L-optimization increases sensitivity by ~ 20 – 60% (the variation is due to nonuniform ^1H density),

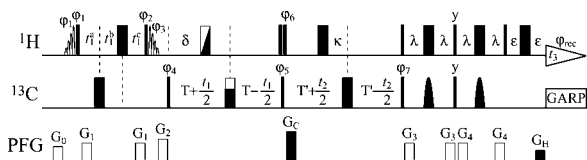


Figure 2. Radio frequency (rf) pulse scheme of L-GFT-TROSY (4,3)D HCCH. 90° and 180° pulses are thin and thick bars. Selective 90° ^1H pulses with rising and falling shapes are 1.1 ms E-BURP2 and time-reversed E-BURP2 pulses¹⁶ applied at 2 ppm. Those flip $^1\text{H}^{\text{aliphatic}}/^1\text{H}_2\text{O}$ magnetization while $^1\text{H}^{\text{aromatic}}$ magnetization is along z . During reverse INEPT, flip-back pulses are not required since (i) hard ^1H pulses yield a 720° rotation of ^1H magnetization and (ii) selective 180° $^{13}\text{C}^{\text{aromatic}}$ REBURP pulses¹⁶ of 610 μs duration (at 750 MHz) decouple $^1\text{H}^{\text{aliphatic}}$ from $^{13}\text{C}^{\text{aliphatic}}$. Phases of ^1H rf pulses are adjusted such that $^1\text{H}^{\text{aliphatic}}/^1\text{H}_2\text{O}$ magnetization is along $+z$ at the beginning of t_3 . Decoupling of $^{13}\text{C}^{\text{aromatic}}$ during t_3 is accomplished using GARP.⁵ Delays: $\lambda = 1.3$ ms, $\kappa = 1.5$ ms, $T = T' = 2.25$ ms, $\delta = T - \kappa + t_1/2$, $\epsilon = 0.3$ ms. Semi- ct $^1\text{H}^{(1)}$ shift evolution⁵ is implemented with $t_{1,\text{max}} = 2T$, $t_1^{\text{a}}(0) = \lambda$, $t_1^{\text{b}}(0) = 1$ μs , $t_1^{\text{c}}(0) = \lambda + 1$ μs , and $\Delta t_1^{\text{a}} = t_1/2$, $\Delta t_1^{\text{b}} = \Delta t_1^{\text{a}} + \Delta t_1^{\text{c}}$, $\Delta t_1^{\text{c}} = -\lambda t_1/2T$. An S^3 -filter¹¹ implements TROSY: the black-and-white 180° pulse on ^1H is applied only every other step of the phase cycle. To decouple $^1\text{J}(^{13}\text{C}^\gamma - ^{13}\text{C}^\beta)$ for enhancing signals at $\Omega(^{13}\text{C}^\gamma)$ in central peak subspectra (Figure 3), the 180° pulse during $t_1(^{13}\text{C}^{(1)})$ is applied with $\gamma B_1 = \Delta\omega/\sqrt{3}$ ($\Delta\omega$ is difference between $^{13}\text{C}^{\text{aromatic}}$ carrier and average $^{13}\text{C}^\beta$ shift). GFT NMR phase-cycle: $\phi_1 = x, y, -x, -y$ to obtain basic subspectra from ^1H and central peak subspectra from ^{13}C polarization.¹² For L-GFT (4,3)D HCCH: $\delta = \kappa$, the black-and-white 180° pulse on ^{13}C during $t_1(^{13}\text{C}^{(1)})$ is at high power and a ^{13}C 90° pulse before PFG G_0 is added (not shown). GFT NMR phase cycle: $\phi_1 = x, y$ for basic subspectra; the central peak subspectrum is recorded by omitting $^1\text{H}^{(1)}$ shift evolution. For definitions of PFGs and phase cycles see Figure S5.

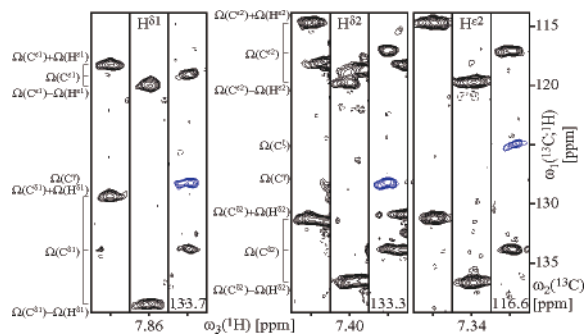


Figure 3. $[\omega_1(^{13}\text{C}^{(1)}), ^1\text{H}^{(1)}], \omega_3(^1\text{H}^{(2)})$]-strips taken along the GFT dimension of L-GFT-TROSY (4,3)D HCCH recorded at 750 MHz for 21 kDa HR41 with $t_{\text{rel}} = 1$ s. Peaks belong to the slowly flipping ring of Tyr 90. Central peaks arising from $^{13}\text{C}^\gamma$ polarization are depicted in blue.

and (iii) $t_{1,\text{max}}(^{13}\text{C}^{(1)}) \sim 4.5$ ms vs 13.5 ms (often required without GFT) increases TROSY sensitivity ~ 2.5 -fold.

HR41 contains 6 Phe, 6 Tyr, and 6 Trp, and nearly complete aromatic resonance assignment²⁰ enabled high-quality NMR structure determination.²¹ Correlation of $^{13}\text{C}^\gamma$ and Tyr $^{13}\text{C}^\epsilon$ shifts with, respectively, $^{13}\text{C}^\delta/^1\text{H}^\delta$ and Tyr $^{13}\text{C}^\epsilon/^1\text{H}^\epsilon$ shifts supports assignment of slowly flipping rings: the same $\text{C}^\gamma/\text{C}^\epsilon$ shifts are detected on $\text{CH}^\delta/\epsilon$ -moieties belonging to an immobilized ring (Figure 3). Nearly complete analysis of ^1H line widths was afforded with (4,3)D HCCH (Tables S6, S7), which is important to explore flipping of all rings in the protein. From ^{13}C -resolved $[^1\text{H}, ^1\text{H}]$ -NOESY,⁵ k_{flip} (Tyr 90) ≈ 0.3 s^{-1} reflects a slow motional mode on the seconds time scale, which proves the absence of faster large-amplitude motions enabling ring flipping. This indicates remarkable rigidity of the substructure in which the ring is embedded. Tyr 90 is conserved among ubiquitin-conjugating enzymes E2 (to which HR41 belongs as inferred from structure^{21b}) and is located in spatial proximity to the interface between E2 and the ubiquitin protein ligase E3.²² Hence, the rigidity and/or the slow motional mode might be important for E2–E3 dimerization and thus for cellular protein degradation.

L-optimization for rapid data acquisition (Figure 1) is exemplified for 13 kDa protein MaR11^{21b} (1 mM; Table S4; Figure S6), an NESG target for which data collection is *sampling* limited.²³ L-GFT (4,3)D HCCH was acquired with $t_{\text{rel}} = 0.3$ s in 25 min (Table S4; 94% peak detection yield).

Overall, for proteins up to ~ 25 kDa, PFG-PEP *ct* L-2D $[^{13}\text{C}, ^1\text{H}]$ -TROSY and L-GFT (4,3)D HCCH are most sensitive, while the TROSY congener is attractive for large proteins and slowly flipping (nearly stalled) rings, which are unique reporters of slow protein dynamics.^{1–3} Aromatic L-optimization includes “flip-back” of $^1\text{H}_2\text{O}$ polarization,²⁴ which is important for systems > 100 kDa.²⁵ We thus expect that L-GFT(-TROSY) (4,3)D HCCH NMR will play a key role for high-quality structure determination of large (membrane²⁶) proteins and for studying the quite unexplored (functional) dynamics of their molecular cores.

Acknowledgment. Support from NIH (P50 GM62413-01) and NSF (MCB 0416899). We thank Drs. G. Montelione and T. Acton for providing samples of PfR13, HR41 and MaR11.

Supporting Information Available: 1. On NMR of aromatic rings. Details of 2. L-optimization, 3. PFG-PEP and TROSY sensitivity enhancement, 4. (4,3)D HCCH, 5. $^1\text{H}^{\text{aromatic}}$ line width analysis for HR41. This material is available free of charge via the Internet <http://pubs.acs.org>.

References

- Wüthrich, K. *NMR of Proteins and Nucleic Acids*; Wiley: New York, 1986.
- Wagner, G. *Q. Rev. Biophys.* **1983**, *16*, 1–57.
- Skalicky, J. J.; Mills, J. L.; Sharma, S.; Szyperski, T. *J. Am. Chem. Soc.* **2001**, *123*, 388–397.
- Kay, L. E.; Ikura, M.; Bax, A. *J. Am. Chem. Soc.* **1990**, *112*, 888–889.
- Cavanagh, J.; Fairbrother, W. J.; Palmer, A. G.; Skelton, N. J. *Protein NMR Spectroscopy: Principles and Practice*; Academic Press: New York, 1996.
- Szyperski, T.; Yeh, D. C.; Sukumaran, D. K.; Moseley, H. N. B.; Montelione, G. T. *Proc. Natl. Acad. Sci. U.S.A.* **2002**, *99*, 8009–8014.
- Pervushin, K.; Vogeli, B.; Eletsky, A. *J. Am. Chem. Soc.* **2002**, *124*, 12898–12902.
- Kay, L. E.; Keifer, P.; Saarinen, T. *J. Am. Chem. Soc.* **1992**, *114*, 10663–10665.
- Pervushin, K.; Riek, R.; Wider, G.; Wüthrich, K. *Proc. Natl. Acad. Sci. U.S.A.* **1997**, *94*, 12366–12371.
- Pervushin, K.; Riek, R.; Wider, G.; Wüthrich, K. *J. Am. Chem. Soc.* **1998**, *120*, 6394–6400.
- Meissner, A.; Sørensen, O. W. *J. Magn. Reson.* **1999**, *139*, 447–450.
- Kim, S.; Szyperski, T. *J. Am. Chem. Soc.* **2003**, *125*, 1385–1393.
- Atreya, H. S.; Szyperski, T. *Proc. Natl. Acad. Sci. U.S.A.* **2004**, *101*, 9642–9647.
- Atreya, H. S.; Szyperski, T. *Method Enzymol.* **2005**, *394*, 78–108.
- PFG-PEP is recommended for all but very large proteins; sensitivity is enhanced up to $\tau_{\text{iso}} \approx 35$ ns (Figure S3) with excellent water suppression. TROSY is generally preferred in 2D *ct* $[^{13}\text{C}, ^1\text{H}]$ -spectroscopy since sensitivity can be enhanced by using $^{13}\text{C}^{\text{aromatic}}$ polarization.¹⁰
- Geen, H.; Freeman, R. J. *Magn. Reson.* **1991**, *93*, 93–141.
- Szyperski, T.; Braun, D.; Banecki, B.; Wüthrich, K. *J. Am. Chem. Soc.* **1996**, *118*, 8146–8147.
- In aliphatic (4,3)D HCCH, central peaks can be derived from ^{13}C polarization since INEPT is tuned for CH, CH_2 , and CH_3 groups.⁵ Aromatic spin systems contain only CH, and delays are tuned to $(1/2J)$. Hence, ^{13}C polarization yields central peaks in aromatic *non*-TROSY (4,3)D HCCH only if sensitivity of basic spectra is compromised.
- Theory predicts that at *ct* delays of 4.5 and 13.5 ms, TROSY becomes more sensitive at $\tau_{\text{iso}} \geq 23$ ns and $\tau_{\text{iso}} \geq 8$ ns, respectively (Figure S4).
- Liu, G.; Aramini, J.; Atreya, H. S.; Eletsky, A.; Xiao, R.; Acton, T. A.; Ma, L. C.; Montelione, G. T.; Szyperski, T. *J. Biomol. NMR* **2005**, *32*, 261–261.
- (a) Shen, Y.; Atreya, H. S.; Liu, G.; Szyperski, T. *J. Am. Chem. Soc.* **2005**, *127*, 9085–9099. (b) Liu, G.; Shen, Y.; Atreya, H. S.; Parish, D.; Shao, Y.; Sukumaran, D. K.; Xiao, R.; Yee, A.; Lemak, A.; Bhattacharya, A.; Acton, T. A.; Arrowsmith, C. H.; Montelione, G. T.; Szyperski, T. *Proc. Natl. Acad. Sci. U.S.A.* **2005**, *102*, 10487–10492.
- (a) Huang, L.; Kinnucan, E.; Wang, G.; Beaudenon, S.; Howley, P. M.; Hübregtse, J. M.; Pavletich, N. P. *Science* **1999**, *286*, 1321–1326. (b) VanDemark, A. P.; Hill, C. P. *Curr. Opin. Struct. Biol.* **2002**, *12*, 822–830.
- With $t_{\text{rel}} = 0.3$ s, the minimal measurement times of L-4D HCCH and L-GFT (4,2)D HCCH¹³ are 4.9 h and 3 min, respectively.
- Grzesiek, S.; Bax, A. *J. Am. Chem. Soc.* **1993**, *115*, 12593–12594.
- Wider, G. *Methods Enzymol.* **2005**, *394*, 382–398.
- Atreya, H. S.; Eletsky, A.; Szyperski, T. *J. Am. Chem. Soc.* **2005**, *127*, 4554–4555.

JA054895X